Connector Response of a Multibody VLFS Subject to Wave Loading

Martijn Hoogeland^{1,*}, Haico van der Werf^{1,2}, Noud Werter¹, and Apostolos Grammatikopoulos²

¹TNO, Department of Structural Dynamics, Delft, NETHERLANDS ²Delft University of Technology, Delft, NETHERLANDS

Abstract. The energy transition requires us to explore all options for generating non-fossil energy and offshore floating PV(OFPV) energy is gaining momentum with recent developments quite promising. The trend is to combine small individual floaters into a grid using connectors which can be made reasonably flexible. To address the challenges of offshore conditions the connectors need strength and flexibility. In this paper, the authors address the challenge of the conflicting demands of strength and flexibility for offshore floating structures. The first step is to assess the wave excitation loads between individual elements and how these loads influence the flexibility of a connection. A computational model is developed that uses a 3D BEM (Boundary Element Method) to calculate the linearized hydrodynamic coefficients and the wave diffraction and radiation forces. Meanwhile, the Froude-Krylov, hydrostatic, connector, and mooring forces are time and spatially dependent allowing nonlinearities to be captured. The time domain solution provides answers into the nonlinear interaction between the mechanical behaviour of compliant (flexible) connectors with hydromechanic behaviour of rigid floaters. After a successful validation, a three-floater OFPV system is subjected to typical sea-states representing 1 year and 100 year return on periods. The pitch motion response is compared for both sea-states and wave headings. Then, the forces and moments at the connectors are presented for two connector stiffnesses and sea-states. The head sea case has the greatest force in the axial direction and moment in vertical bending but then the forces and moments in the other DOF are greater in bow quarter seas. There is a decrease in forces but increase in moments when the stiffness of the connectors increases. The results also show the importance of dynamic amplification at sea-states with wave peak periods close to the natural frequency of the system. The connectors are shown to influence the natural frequency of the structure such that it behaves somewhere in between a single continuous structure and three independent floating modules. After successfully using the model to investigate the behaviour of a serially connected OFPV the next step will be to expand to a grid which is more representative of the future types of structures that will be deployed.

Keywords: Offshore Floating Solar, multibody, fluid-structure interaction, VLFS

1. Introduction

Recent international agreements, such as the Glasgow Climate Agreement are pushing the energy industry to expand the use of renewable sources to meet high decarbonization goals. In order to achieve this, there is a growing interest in expanding current energy production facilities offshore due to the increasing space limitations associated with human expansion and limited arable lands around population centers. One innovative solution being proposed is to construct floating solar islands, Offshore Floating PV (OFPV). To practically contribute to the energy transition these islands are likely to become VLFSs (Very Large Floating Structures). The benefit of such a structure is that it does not require space onshore and that it can be installed between offshore wind installations and utilize some of its infrastructure such as power transmission stations or seabed mooring locations.

A VLFS is usually so large that its motion in waves cannot be described as a single rigid body and alternative models must be used [1]. The VLFSs as OFPV can be broadly categorized into two types: the joint-type and the mat-type. The joint-type usually consists of elaborate and stiff structures, such as semi-submersible platforms which are connected together by mechanical connectors [1], and are designed to be deployed offshore. Alternatively, the mat-type usually consists of flexible components and has a shallow draft. An OFPV system can fit into either of these categories depending on the design. The SolarDuck concept suits the joint-type description

1

^{*} Correspondence to: martijn.hoogeland@tno.nl

with many triangular shaped barges (floaters) [2]. Alternatively, the concept by Schrier and Jacobi [3] proposes a mat-type VLFS intended for offshore conditions.

There were a few large research programs such as the TRAM Megafloat, USA MOB (Mobile Offshore Base), and Chinese MOB projects which have all led to significant advances in understanding the dynamic behavior of these specific types of structures [4]. In contrast, projects relating to floating solar have seen some interest, but there is limited amount of publicly available research. Floating solar structures behave differently to the MOB or runway designs because the displacements of the floaters are not restricted. Generally, an OFPV system must be easy and low-cost to build and install while surviving harsh ocean conditions. Consequently, they are designed to be simple, light and modular. Consisting of many individual floaters, there are numerous connectors and optimizing the design saves costs for the entire system. Efficient design must include reliability, hence the longevity as well as the ultimate strength should match and have similar safety factors.

This paper will describe how a numerical model is used to simulate the connector response of an OFPV system in a wave spectrum. Firstly a summary of the work of other researchers and different calculation methods is presented. Then, a three floater model is proposed which is connected in a serial pattern using beam elements with linear stiffness in five degrees of freedom. The results and discussion will address the relationship between connector compliance and the floater motions and the difficulties in providing reliable predictions. This paper is part of on-going research into determine the hydrodynamic and structural behavior of an OFPV.

2. Motivation

Previously the behavior of a VLFS has been researched using the theory of hydroelasticity. Hydroelasticity is the study of the elastic behavior a structure in a fluid and was first pioneered by Bishop and Price [6] who investigated the harmonic response of ships using 2D beam theory and a 2D strip theory method. The structural response prediction in various investigations is based on elastic plate theories such as: Kirchhoff plate theory for thin plates [7], Mindlin first order shear deformation theory if length to depth ratio increases [8] and Timoshenko beams if this ratio increases further still [1]. These methods can be accurate but are specific to cases where the structural stiffness is linear and deformations remain small [9].

Hydroelasticity is also studied using computational methods which combine linear strip theory or BEM (Boundary Element Method) with a structural solver using FEM (Finite Element Method) or 2D beam theory. Linear potential flow based hydrodynamic models are often adopted because they can be computed relatively fast and provide reasonable accuracy [10]. Linear models can be computed in the frequency domain which reduces computational time and assume linear superposition of regular waves to form the response in a specific sea state.

Advances in research have improved the understanding of the behavior of a VLFS due to nonlinear structural responses such as nonlinear stiffness, geometries, nonlinear motion responses due to large displacements, or non-rectangular plan shaped geometries. When the relative displacements of the structure becomes large it can become necessary to solve the equation of motion in the time domain to capture nonlinearities associated with connector and floater interaction. This was demonstrated by Zhang et. al. [11] who used a network modelling method to show nonlinear dynamic effects on a multi-body VLFS in irregular waves at various wave headings. The non-rectangular geometries most studied are circular [12], [13] followed by L, X or T plan shapes [14]. Changes in geometry has a large effect on the hydrodynamic forces experienced by the structure due to the refraction angle. This can be beneficial when the wave environment becomes more multidirectional and oblique.

For the research presented in this paper, the OFPV is described using a multi-body solution because the floaters are quite independent from each other. The multi-body approach seems be more suited for a joint-type VLFS because this can simplify the calculations by solving one equation of motion for all the floaters [11], [15]. It has also been shown that the hydroelastic effect for relatively stiff modules can be correctly introduced by assuming rigid floaters and flexible connections [16], greatly decreasing computational cost.

A multi-body approach can be used to study the dynamic motion of a VLFS in waves. Often the joint-type VLFS has been modelled assuming the floaters are rigid, and the flexibility is only found in the connectors. In the present investigation, if the connection allows movement in a prescribed degree of freedom (DOF) but is rigid in others then it is described as a 'kinematic connection' (such as hinged) while if there is a finite stiffness in one or more DOFs, this is a 'compliant connection'. A compliant connector model was used for this research.

The concept of a compliant connector was first developed by NASA [17] and was later adopted by Derstine and Brown [18]. The design was developed for an offshore multi-modular military base which could allow small deformations in some DOFs but larger deformations in others. This was shown to reduce overall connector loads compared to a pure kinematic hinge joint. Hinges can only change in direction of movement, and stiffness or damping. Introducing compliant connectors can be done by, amongst other, springs [18], rubber and cable [9], air cushion and cable [19], or hydraulic, fender and elastomer bearing [20] combinations. A compliant connector makes the system design more complicated to accurately predict its behavior because of the complex interaction with the modules response.

The current numerical models proposed in literature assume simple connections namely, kinematic hinges which can freely rotate in one DOF. However, there is a wide range of types of connectors at the disposal of a designer, which are ignored in most investigations. For the solar concept, the compliant connectors are ideal because the stiffness can be controlled in all DOFs and compliance can help reducing the maximum forces and moments occur between individual platforms. An assessment of a multi-body structural interaction in waves with compliant connectors has not been thoroughly investigated.

The connectors of a OFPV system are critical elements of the structural design regarding both ultimate strength and fatigue life. A greater knowledge of the connection allows a greater understanding of the loads which allows safety margins when designing them. Increasing the knowledge of the margin between loads and structural limits of a connector improves the design, lead to reduced costs for maintenance, and provides greater confidence to the industry for investment.

The connector characteristics such as, the stiffness, damping and DOFs, play an important role in the overall response of the structure because they influence the floater motions and connector loads [4]. Initial designs of a VLFS with rigid connections led to excessive forces developing at the connectors which are significantly reduced when there is a flexibility introduced [21]. Further studies showed that the motions of the floaters and the forces at the connectors are influenced by varying the stiffness of the connectors [22]. Varying the level of damping also has an influence on VLFS motions [23] however, this has been largely ignored by most researchers.

It can be difficult to numerically model the structure's motion responses because the complex multi-body interaction results in convergence issues. This type of phenomenon was identified by Zhang et. al. [11] and then extended by Xu et al. [24] who developed nonlinear stiffness models to determine the connector behavior in a MOB structure. It became apparent that at certain wave frequencies the structure experienced resonance which was termed as the 'amplitude of death' because it would result in an unstable system response.

Most of the current research found on joint-type VLFSs have the modules connected serially. The designs have the connector acting in one direction which can reduce stresses in pitch if the modules are in-line and head or following waves are experienced. However, if the waves are irregular and/or oblique to the structure, this might manifest new critical modes or load combinations when modules are connected in a grid pattern. This might influence the design of the structure and/or mooring arrangement. The plan shape of a module might be able to reduce connector stresses in governing wave conditions.

There is an interdependence between the motion response of the modules and the deformation experienced by compliant connectors. The situation becomes even more complicated when nonlinearities are introduced in the connectors' behavior. For many compliant connectors, the stiffness cannot be assumed to behave linearly with the displacement. This interaction has not been researched in detail because it requires nonlinear solvers with high computational cost. Most recent studies on MOB structures assumed that the relative displacements between modules are reasonably small, so that the nonlinearities become negligible however, the equation of motion must be solved in the time-domain if displacements become large.

3. Hydrodynamic & Structural Modelling

The numerical tool that has been used to perform this research was developed by Tuitman [25]. This will be described in this section. The multi-body hydrodynamic problem is implemented using a 3D boundary element method (3D-BEM) and solving the equation of motion with compliant constraints. The present method assumes that the fluid problem is continuous, inviscid, incompressible, non-rotational and initially uniform. In this way, the

solution is linearized such that the fluid velocity can be described using potential theory where the Laplace equation is used to solve for the velocity potential (φ) shown in equation (1).

$$\Delta \varphi = 0 \tag{1}$$

'Airy waves' are assumed such that wave non-linearities are ignored which allows the use of linear superposition. It is possible to apply potential theory to describe the seakeeping behavior of a floating structure in waves if nonlinear hydrodynamic behavior which occur due to viscous damping, shallow water effects and/or body interaction is small [26]. Linear superposition allows the regular, sinusoidal waves with a certain height and phase angle constituting a wave spectrum to be used to calculate the response spectrum.

The hydrodynamic coefficients are first calculated in the frequency domain using the 3D-BEM described by Tuitman [25]. This requires generating a hydrodynamic mesh which is reasonably consistent and small enough to capture frequencies up to 3 rad/s. The maximum panel size needed to achieve a stable solution is proportional to the wavelength [25]. The hydrodynamic mesh was generated using the open-source program GMSH. The mesh requires integrating over the entire wetted surface and must be defined up to the still water free surface boundary.

The hydrodynamic coefficients describe the fluid motion around the floater and are needed to solve the equation of motion. These coefficients are computed in the frequency domain to reduce the simulation time, however this means that nonlinear effects are not captured using this method. The added mass and hydrodynamic damping are frequency-dependent while the spring stiffness (restoring coefficient) is frequency-independent.

The wave potentials can be divided into an incident, diffracted and radiated component such that:

$$\varphi = \varphi_I + \varphi_D - i\omega \sum_{j=1}^N \vec{\xi}_j \cdot \varphi_{R_j}$$
 (2)

Where φ is the total velocity potential, φ_I is the incident potential, φ_D is the diffracted potential, ω is the wave frequency, N is the number of degrees of freedom, ξ is the wave elevation, and φ_R is the radiated potential. The diffracted and radiation velocity potentials are solved using the following boundary conditions.

$$\begin{cases} \Delta \varphi = 0 & \text{In the fluid,} \\ -k\varphi + \frac{\partial \varphi}{\partial z} = 0 & z = 0, \\ \frac{\partial \varphi}{\partial \vec{n}} = V_n & \text{On } S_b, \\ \lim \left[\sqrt{kR} \left(\frac{\partial \varphi}{\partial R} - ik\varphi \right) \right] = 0 & R \to \infty \end{cases}$$
 (3)

Where, V_n is the normal velocity potential, k is the wave number, z is depth, S_b is the wetted surface, n is a normal vector to the surface, R is the distance to a body fixed origin. This boundary value problem is solved numerically at the center of the mesh elements using Green's source functions. The pressures are then obtained using linearized Bernoulli equation shown in equation (4).

$$P = i\omega\rho\phi \tag{4}$$

Where the pressure (P) is calculated for the respective potentials. Here ρ is the water density which is assumed constant. The force is then obtained by integrating the pressure over the wetted surface. The incident wave force and hydrostatic force are combined in equation (5) and are displacement and time dependent. The radiation potential must be calculated from the added mass and damping coefficients.

$$f_{I,i} = \iint_{S_B} (P_I(t, x_{pos}) + P_{HS}(t, x_{pos})) \vec{h}_I \vec{n} \, dS$$

$$f_{D,i} = \iint_{S_B} P_D \, \vec{h}_I \vec{n} \, dS$$
(6)

$$f_{D,i} = \iint_{S_B} P_D \, \vec{h}_I \vec{n} \, dS \tag{6}$$

$$\omega_e A_{ij} + i\omega_e B_{ij} = \iint_{S_R} P_{R_j} \vec{h}_I \vec{n} \, dS \tag{7}$$

Where, $f_{\rm I}$ is the addition of the nonlinear incident (Froude-Krylov) force, f_{HS} is the nonlinear hydrostatic force, $f_{\rm D}$ is the linearized diffraction force, A is the linearized hydrodynamic added mass and B is the linearized hydrodynamic damping. The components of the wave forces and hydrodynamic coefficients are calculated when all free floating bodies are interacting in the fluid domain but before constraints and moorings have been attached. This is currently a limitation of the model because these constraints might influence the radiation potentials.

The total exciting forces are then combined in equation (8).

$$F_i = f_{\rm I} + f_{\rm grav} + f_{\rm beam} + f_{\rm moor} + f_{\rm R} + f_{\rm D} \tag{8}$$

Here F_i is the total force in DOF 'i', f_I is the Froude-Krylov and hydrostatic forces combined, f_{grav} is gravity force, f_{beam} is beam element, f_{moor} is the mooring force, f_R is the radiation force, and f_D is the diffraction force.

The force in the beam is calculated using linear Euler-Bernoulli beam theory in all 6 DOFs. A single linear beam element is generated between two nodes on the floating bodies.

$$f_{heam} = k * u$$

The equation of motion is solved in the time-domain because the connector reaction forces are displacement dependent, not frequency dependent. The equation of motion of an object floating in regular waves can be described using equation (9). This is solved using a 4th order Runge-Kutta numerical time-integration scheme as described in [25].

$$F_{i} = (M_{i,i} + A_{i,i}) \cdot \ddot{x}_{i} + B_{i,i} \cdot \dot{x}_{i} + C_{i,i} \cdot x_{i}$$
(9)

The equation of motion is then transformed to the time domain using the Cummins equation which is a commonly used method to convert from frequency domain using impulse theory [27]. The added mass (A), and the damping (B) that have been initially calculated in the frequency domain are transformed to the time domain using equation (10). The frequency independent terms such as the mass (M) and stiffness matrices (C) remain constant. Force relates to the displacement (x) and its derivatives in time for velocity (x) and acceleration (x).

$$\sum_{j=1}^{6} \{ \left(M_{i,j} + A_{i,j} \right) \cdot \ddot{x}_{j}(t) + B_{i,j}(\omega_{\infty}) \cdot \dot{x}_{j}(t) + \cdots \\ \dots \int_{0}^{\infty} K_{i,j}(\tau) \cdot \dot{x}_{j}(t - \tau) \cdot d\tau + C_{i,j} \cdot \dot{x}_{j}(t) \} = X_{i}(t)$$
(10)

The radiation force can be calculated using.

$$f_R = B_{i,j}(\omega_\infty) \cdot \vec{\xi}(t) + \int_{-\infty}^t C_{i,j}(t-\tau) \cdot \vec{\xi} \, d\tau \tag{11}$$

The external, time-dependent exciting force is given by $X_i(t)$. The added mass and damping terms can be converted by the introduction of a retardation function (K) which describes the response delay from the impulse load over time. The damping coefficient at infinite frequency cannot be obtained using 3D-BEM; hence, the value at the maximum calculated frequency is used. The retardation function is given by equation (12).

$$K_{i,j}(t) = \frac{2}{\pi} \cdot \int_0^\infty (B_{i,j}(\omega) - B_{i,j}(\omega_\infty)) \cdot \cos(\omega \cdot t) \cdot d\omega$$
 (12)

And the added mass term becomes.

$$A_{i,j} = a_{i,j}(\omega_{\infty}) + \frac{1}{\omega_{\infty}} \cdot \int_{0}^{\infty} K_{i,j}(\tau) \cdot \sin(\omega \tau) \cdot d\tau$$
 (13)

However, given that the expression can be valid for infinite frequencies, the expression can be simplified to.

$$A_{i,j} = a_{i,j}(\omega_{\infty}) \tag{14}$$

Careful attention should be paid here because this assumption is only valid if the coefficients are calculated at frequencies sufficiently high that the response functions (calculated at equation (8)) tend to zero, which in this analysis is 5 rad/s. This requires a small panel size in the hydrodynamic mesh which might result in extremely long computations computational time if the VLFS becomes very large, such as when there are many modules. The solution to this problem is to perform a hydrodynamic analysis up to a sufficiently high frequency and then perform interpolation using an appropriate function [25].

4. VLFS Design and Wave Characteristics

The VLFS design inputs and environmental conditions are presented in this section. The VLFS consists of three serially connected identical box barges as shown in Figure 1. The floater size is indicative and based on pilot offshore floating solar projects. The floater dimensions and properties are given in Table 1. There are 4 mooring lines attached to the forward and aft floater. The purpose of the mooring stiffness is to prevent the structure from drifting away and a constant stiffness value of 1E+04 N/m was selected to avoid interference with the motion of the structure. A water density of 1025kg/m³ is used for the fluid domain.

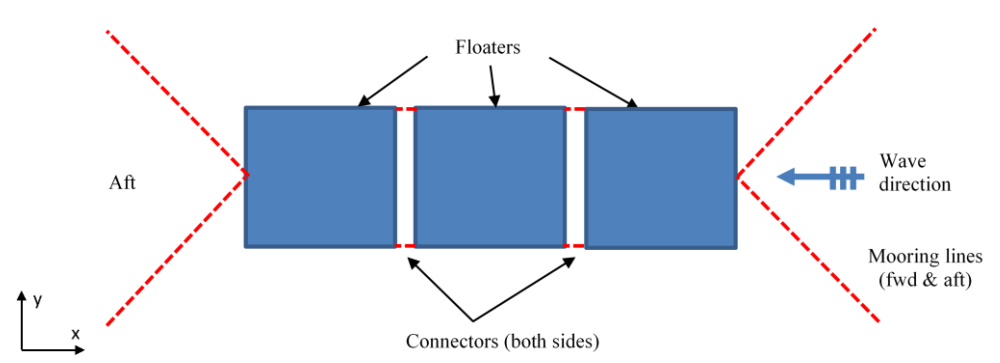


Figure 1. VLFS arrangement (plan view).

Table 1. Physical properties of single floater.				
Length	15.0 m			
Breadth	15.0 m			
Draft	1.0 m			
Module gap	2.0 m			
I_{xx}	8.65 E+06 kg.m ²			
I_{yy}	4.34 E+06 kg.m ²			
I_{zz}	4.34 E+06 kg.m ²			

Table 1 Physical properties of single floater

The connectors are compliant in multiple DOF such that a flexible connector rigid module (FCRM) model is assumed. Connectors are idealized as massive rods, having axial and bending stiffness. There are two connectors between each of the floaters with lengths of 2m. The stiffness values are derived from equations for Euler beams in bending and compression or tension for an arbitrary solid steel rod of a radii 90, 130 and 150mm. The stiffness of the compliant connectors is defined assuming a 12x6 stiffness matrix as shown in Table 2 for a medium stiffness connector. The yaw moment is ignored because the port and starboard surge restraints resist this rotational motion.

The analysis is performed using data for the 1- and 100-year extreme wave conditions in the Hollandse Kust (Noord) location, which has been selected for offshore energy development by the Dutch Government. The

significant wave height (H_s) , wave period (T_p) , and gamma have been obtained online [5]. A typical condition with 1 (SS-A) and 100 (SS-B) year return period is chosen. The values used are shown in Table 3. The wave headings are chosen as 90 (beam seas), 120 (beam quartering), 150 (bow quartering) and 180 degrees (head seas). A time trace representing the sea state has been generated using the JONSWAP formulation of the spectrum to represent ocean conditions for 1000 seconds, which is approximately one return period for 300 wave components. This number is chosen because it ensures repeatability when analyzing the statistical results.

Table 2. Example stiffness matrix for medium stiffness (130mm solid steel rod) compliant connectors.

	x (N/m)	y (N/m)	z (N/m)	rx (Nm/rad)	ry (Nm/rad)	rz (Nm/rad)
X	1.33E+09	0	0	0	0	0
Y	0	6.73E+07	0	0	0	0
Z	0	0	6.73E+07	0	6.73E+07	0
Rx	0	0	0	6.73E+07	0	0
Ry	0	0	6.73E+07	0	8.97E+07	0
Rz	0	0	0	0	0	0
X	-1.33E+09	0	0	0	0	0
Y	0	-6.73E+07	0	0	0	0
Z	0	0	-6.73E+07	0	-6.73E+07	0
RX	0	0	0	-6.73E+07	0	0
RY	0	0	6.73E+07	0	4.49E+07	0
RZ	0	0	0	0	0	0

Table 3. Input JONSWAP irregular wave conditions.

		1 Year Extreme (SS-A)	100 Year Extreme (SS-B)
Significant wave height (m)	H_{S}	5.6	7.6
Wave peak period (sec)	T_p	10.0	11.8
Gamma (-)	γ	3.3	3.3

5. Results and Discussion

5.1. Validation

The results from the numerical model are presented and discussed in this section. First the model is validated against an existing experiment and then the responses of the 3 floater model described in Section 3 has been shown for two sea-states. Initially numerical results have been compared with the experiment presented by Remy et al. [28]. Their experimental setup with 12 connected box-barges is numerically modelled using the inputs provided in the paper. The results show the motions for heave, pitch and roll for 0- and 90-degree regular waves. The motions are an average of all the floaters taken at their individual centers of gravity. The bending moment is taken as the average of the pitch moment at the connectors located at midships for head waves.

The numerical calculations performed using this numerical solver are compared to the experimental results by Remy et al. [28], who presented for heave, roll, and pitch see Figure 2. Validation is performed to assess the accuracy of the numerical 3D-BEM as well as the beam connector model against physical experiments. In general, there is a good correlation between the numerical prediction and experimental result. There is some uncertainty in both the experimental and numerical results. The RAOs are retrieved from time signals, using the input wave spectrum. Such process is prone to disturbances being picked up. The numerical results have inherent uncertainty due to discretization errors and calculating the hydrodynamics using an inviscid solver. The RAOs are retrieved form response signals calculated using a numerical wave spectrum, hence without disturbances. Nonlinear radiation effects are not included, generally resulting in smooth curves.

The numerical and experimental results have also been compared for the bending moment as shown in Figure 3. The results have been calculated for the highest bending moment which occurs at the center of the 12 floaters as tested by Remy et al. [28] (amidships of the entire structure). For the numerical result the bending moment in the 'numerical beam' case is taken at the connectors joining floater 6 and 7 whereas, for the 'numerical pitch' and the experimental cases the pitch displacement of the forward and aft floater are used to derive the bending moment with Euler beam equations. The numerical results align well with the experiment however, for wave periods

between 1.1 and 1.6 seconds the numerical beam result is slightly lower. The results indicate that the magnitude of the bending moment varies depending on how the measurement is taken.

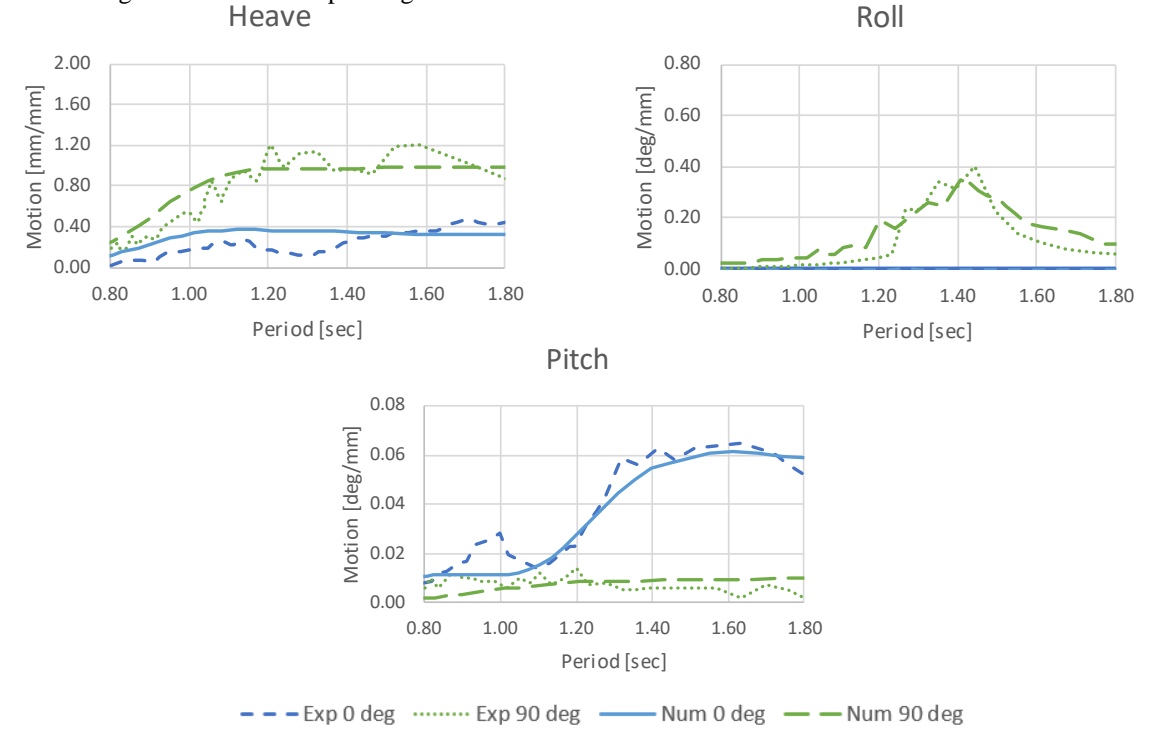


Figure 2. Motion RAOs for heave, roll and pitch with experimental results for head waves (*medium dashed line*) and beam waves (*dotted line*) and numerical results for head waves (*solid line*) and beam waves (*longer dashed line*).

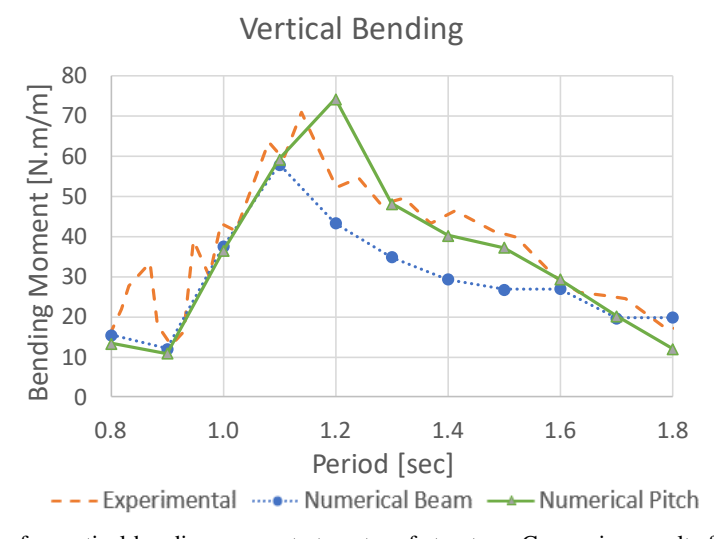


Figure 3. Forced response for vertical bending moment at center of structure. Comparing results for numerically calculated based on bending at beams (*dotted line circles*), numerical calculated from pitch displacement (*solid line dots*), and experimental calculated from pitch displacement (*dashed line*).

5.2. Example Case

The 3 floater VLFS described in Section 4 was numerically modelled, and motions calculated in the time-domain using 3D-BEM. The motions are obtained in the time domain as shown in Figure 4 for pitch in SS-A and SS-B, for the mid floater with medium stiffness connectors. The RMS values of the time signal in SS-A are presented in Figure 5. The largest pitch motion is recorded for head waves (180 degrees) with the least stiff connector configuration. There is a clear decrease in the motions as the connector stiffness increases from soft to the stiffest configuration. The connector stiffness has the largest effect on pitch motion of approximately 35%

difference compared to the other DOF which had a maximum of 8% in surge which is why only the significant pitch motion has been presented.

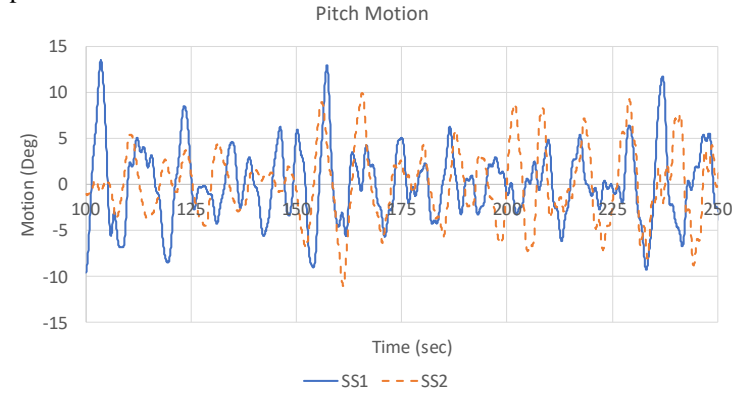


Figure 4. Pitch motion of mid floater through time for SS-A (solid line) and SS-B (dashed line).

It is interesting to note that the relative motions between the floaters vary considerably when the connectors are less stiff. The aft floater has a higher pitch motion in all cases whereas the middle floater has the lowest. The difference between the relative motion reduces as the beam stiffness increases. In head seas the maximum difference between the floaters is 15% and 6% for the soft and stiff connector cases (respectively). This is expected as the whole structure will tend to behave like a single rigid body as was also demonstrated by Xia et. al. [29].

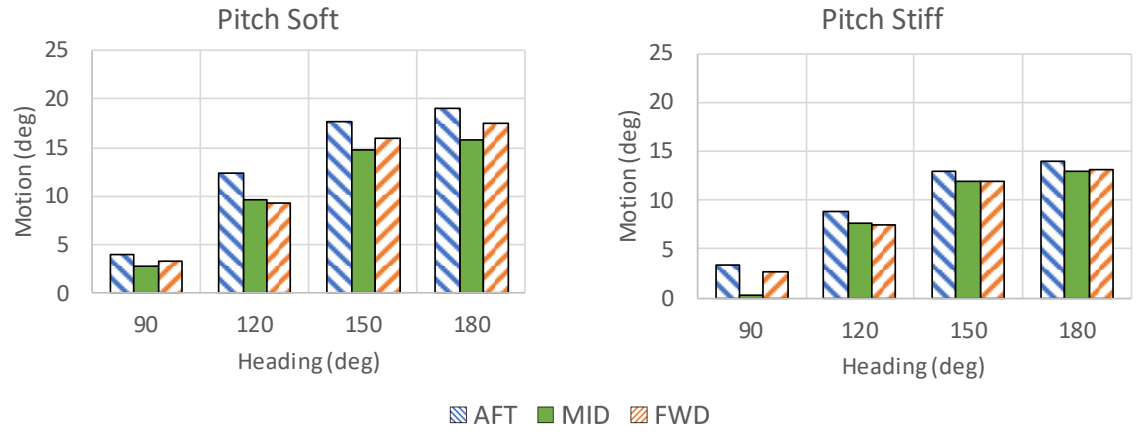


Figure 5. RMS pitch motion for three floaters aft (*left column*), mid (*middle column*), and aft (*right column*) at various wave headings. The results are shown for two stiffness configurations soft (*left*) and stiff (*right*). The sea-state with 1 year return period (SS-A) is used to generate the irregular wave spectrum.

The internal forces and moments at the compliant connectors have also been investigated in this study. The results in Figure 6 show the averaged values from each connector and at each wave heading (90, 120, 150, and 180 degrees). The error bars show the maximum and minimum values for all the connectors. The connector stiffness appears to have a profound effect on the forces and moments developed in the connectors. Forces generally decrease with increasing stiffness apart for heave in SS-B which increases significantly. The roll and pitch moments both increase. The maximum for Fx and My occur in head seas while for the other DOF the 150 degree (bow quartering) seas give the maximum results.

The differences between the averaged forces and moments experienced by the soft and stiff connectors in all DOFs are quite high. This variation is not linearly proportional to the corresponding motions as only the pitch motion tends to decrease significantly when the stiffness increases. This suggests that, for this arrangement, pitch motion dictates the forces and moments in the connectors. Furthermore, both aft connectors have lower forces and moments than the forward pair which coincides with the aft floater experiencing larger (pitch) motions. The forces developed from the higher sea state decrease which could be attributed to the shift in the JONSWAP peak period away from the structure's natural frequency. The pitch and roll moments both increase from SS-A to SS-B.

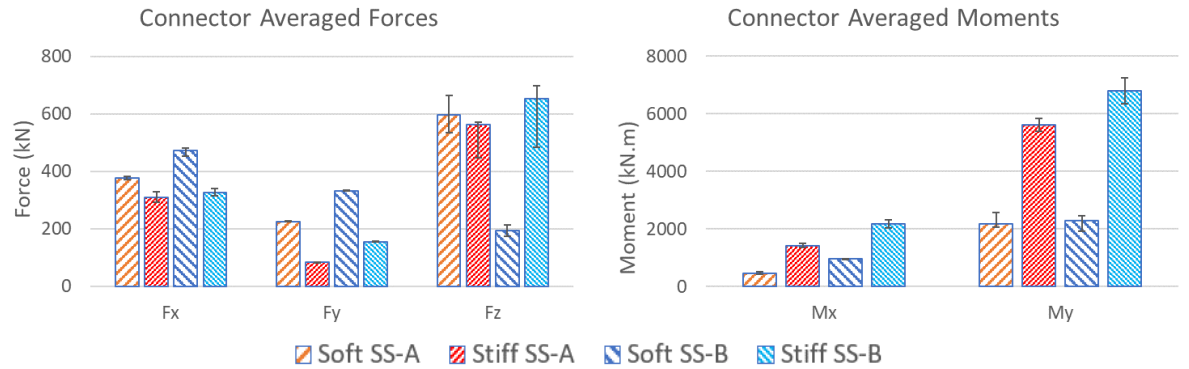


Figure 6. The internal connector forces (*left*) and moments (*right*) taking averages from all connectors at all wave headings analyzed (90, 120, 150, and 180 degrees) for SS-A and SS-B. The soft and stiff connector responses are presented. Error bars show maximum and minimum force or moment from all of the connectors.

The pitch response function for the middle floater is also presented in Figure 7 which is obtained by calculating the peak pitch motion for 1m wave height regular head waves at nine regular frequencies for the three floater model with medium stiffness connectors. The aft floater is presented but the variation between the three floaters did not change significantly and at the peak has a maximum difference of 12%. There is a distinct peak in the response function signifying that resonance might occur at an excitation frequency of approximately 1.2 rad/s, similar to 5 second peak period. The pitch motion for 1m waves is 1.5 degrees at this wave frequency.

The connector model VLFS has been compared with a case where there are three free floaters with no connections, and one continuous structure which is equal in length to the three floater model and gaps, reflecting on the response function for pitch. The result shows that the addition of connectors shifts the natural frequency of the structure and magnitude of the peak motion to somewhere in between the free and continuous case (1.67- and 0.92 rad/s respectively). By separating the structure into multiple smaller floaters with connectors, the resonant frequency is shifted away from the wave spectral peaks of SS-A and SS-B (0.62- and 0.49 seconds respectively) but also the magnitude of the peak is reduced for a structure that has the same surface area.

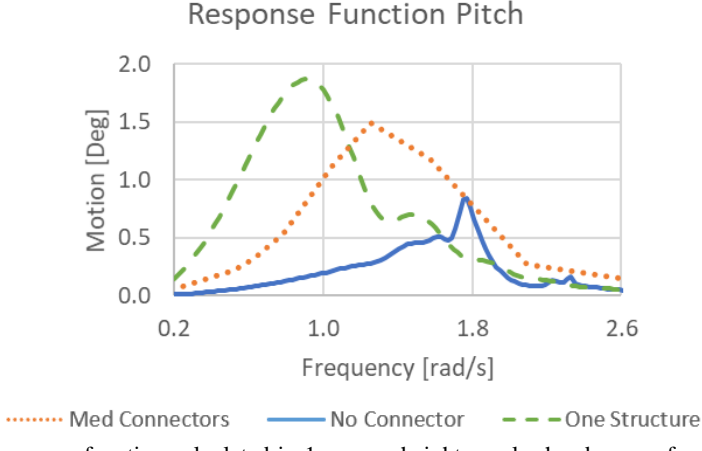


Figure 7. Pitch motion response function calculated in 1m wave height regular head waves for the three floater model (aft floater shown) with medium stiffness connectors (*dotted line*), no connectors (*solid line*), and one structure (*dashed line*).

6. Conclusions and Recommendations

In this paper, a numerical method model has been developed which simulates a concept VLFS as OFPV system in irregular waves, assuming rigid floaters and compliant connections. There are multiple floaters which have been connected using beam elements with linear stiffness characteristics. A 3D-BEM model was used to solve for frequency dependent hydrodynamic coefficients. The compliant connectors were defined by a stiffness matrix. The system was exposed to wave excitation forces and the equation of motion was solved in the time-domain to capture nonlinear behavior associated with the interaction of structural behavior of the connectors and the hydrodynamic response of the floaters.

The numerical analysis was validated against an experiment with 12 box floaters conducted by Remy et. al. [28]. The motions were compared in heave, roll, and pitch and the agreement was good. The bending moment generated at the connectors between the centermost floater (numerical) are compared to the bending moments derived from the difference in pitch of the forward and aftmost floaters (experimental and numerically). The numerical results calculated at the beams are slightly lower for the higher frequencies compared to the results when calculated using the relative pitch motion. Comparing the pitch moments numerical and experimentally at the same floaters, gave satisfactory results.

A representative system consisting of three 15x15x2 m floaters with compliant connectors was analyzed in two sea-states and 4 headings, representing 1 and 100 year return period conditions, ranging from beam to head seas. Each floater is connected by two connectors with compliance in 5 DOFs and the system is soft moored. The stiffness of the connector appears to have a strong influence on the pitch motion which decreases significantly when stiffness increases. The comparison of the internal forces and moments show that as stiffness increases, the forces decrease, while the moments in roll and pitch both increase. The reduction in translational forces is a result of the peak period of 100 year return period sea state being shifted further from the natural frequency of the structure as seen in the pitch response function analysis. Additionally, the reduction is also a result of the load being resisted by the bending moment developed in the connector. The head seas case has higher axial forces and vertical bending moments whereas the bow quartering has greater forces and moments in the other DOF.

There is a shift in the frequency where the peak pitch motion occurs when comparing to three free floaters and the single continuous structure. The pitch response function shows that the natural excitation frequency is approximately 1.25 rad/s which is between the continuous structure (0.92 rad/s) and the free single floater (1.67 rad/s). Furthermore, the magnitude of the peak motion of the three floater model at the resonant frequency is between the two other cases. The dynamic, mechanical, response of the connector is dominant over the hydrodynamic response of the floaters when the peak period of the wave spectrum is close to the excitation frequency of the structure. This dynamic effect means that static or quasi-static analysis cannot be used to predict the connector forces and moments or floater motions.

The method has only be applied on a serial arrangement of floaters and connectors, with satisfactory results. The method needs to be expanded to a grid-like structure, because OFPV systems deployed offshore will consists a multiple rows and columns of individual floaters. There is a potential that other DOFs, not pitch, become critical to the system response in waves. In particularly, the dynamic amplification of individual floaters in a grid pattern may show large variations. Furthermore, analyzing different shaped floaters would give interesting results. For instance triangular floaters will have other response to heading variation compared to orthogonal systems. The compliant connector model can also be improved to introduce damping and nonlinear spring stiffness.

References

- M. Lamas-Pardo, G. Iglesias and L. Carral, "A review of very large floating structures (VLFS) for coastal and offshore uses," Journal of Ocean Engineering, vol. 109, pp. 677-690, 2015.
- Solar Duck, "Solar Duck," 2021. [Online]. Available: https://solarduck.tech/.
 S. Schreier and G. Jacobi, "Measuring hydroelastic deformation of very flexible floating structures," in 2nd World Conference on Floating Solutions, Rotterdam, Netherlands, 2019.
- H. Suzuki, M. Fujikubo, H. R. Riggs and Y. Yasuzawa, "Very large floating structures," Southampton, UK, 2006. [4]
- Fugro and Deltares, "Hollandse Kust (noord) Field Measurement Campaign," 2017. [5]
- [6] R. E. D. Bishop and W. G. Price, "Hydroelasticity of ships," Cambridge University Press, 1979.
- M. Kashiwagi, "A B-spline Galerkin scheme for calculating the hydroelastic response of a very large floating [7] structure in waves," Journal of Marine Science and Technology, vol. 3, pp. 37-49, 1998.
- S. Wang, R. C. Ertekin, A. T. F. M. van Stiphou and P. G. P. Ferier, "Hydroelastic response analysis of a box-like floating airport of a shallow draft," The Hague, Netherlands, 1995.
- H. Zhang, D. Xu, C. Lu, E. Qi, C. Tian and Y. Wu, "Connection effect on amplitude death stability of multimodule floating airport," Ocean Engineering, vol. 129, pp. 46-56, 2017.
- I. V. Struova, "Diffraction of shallow-water waves on a floating elastic platform," Journal of Applied Mathematics and Mechanics, vol. 64, pp. 1004-1012, 2000.
- H. Zhang, D. Xu, S. Xia and Y. Wu, "A new concept for the stability design of floating airport with multiple modules," in IUTAM Symposium on Nonlinear and Delayed Dynamics of Mechatronic Systems, Nanjing, China, 2017.
- K. Takagi and M. Nagayasu, "Hydroelastic behavior of a mat-type very large floating structure of arbitrary [12] geometry," Honolulu, USA, 2001.
- M. H. Meylan, "The wave response of an ice floe of arbitrary geometry," Journal of Geophysical Research Atmospheres, vol. 107, no. C1, pp. 5.1-5.11, 2002.

- T. Hamamoto and K. Fujita, "Wet-mode superposition for evaluating the hydroelastic response of floating [14]
- structures with arbitrary shape," Kitakyshu, Japan, 2002.
 [15] R. C. Ertekin and H. R. Riggs, "Efficient methods for hydroelastic analysis of very large floating structures," Ship Research, vol. 37, no. 1, pp. 58-76, 1993.
- J. Kerley, W. Eklund, R. Burkhardt and P. Rossoni, "Cable compliance, NASA technical paper 3216," NASA Goddard Space Flight Center, 1992.
- M. S. Derstine and R. T. Brown, "A compliant connector concept for the mobile offshore base," Marine Structures, [17] vol. 13, pp. 399-419, 2000.
- Q. Shi, D. Xu, H. Zhang, H. Zhao, J. Ding and Y. Wu, "A face-contact connector for modularized floating [18] structures," Marine Structures, vol. 82, 2022.
- G. Rognaas, J. Xu, S. Lindseth and F. Rosendahl, "Mobile offshore base concepts Concrete hull and steel topsides," Marine Structures, vol. 14, pp. 5-23, 2001.
- H. Maeda, S. Maruyama and R. Inoue, "On the motions of a floating structure which consists of two or three blocks [20] with rigid or pin joints," Ocean Engineering, vol. 17, pp. 91-98, 1979.

 [21] H. R. Riggs, R. C. Ertekin and T. R. J. Mills, "A comparative study of RMFC and FEA models for the wave-
- induced response of a MOB," Journal of Marine Structures, vol. 13, pp. 217-232, 2000.
- [22] D. Xu, H. Zhang, S. Xia, C. Lu, E. Qi, C. Tian and Y. Wu, "Nonlinear dynamic characteristics of a multi-module floating airport with rigid-flexible connections," Journal of Fluid Structures, vol. 59, pp. 270-284, 2015.
- [23] H. R. Riggs and R. C. Ertekin, "Characteristics of the wave response of mobile offshore bases," St Johns, USA, 1999.
- D. L. Xu, H. C. Zhang, C. Lu, E. R. Qi, C. Tian and Y. S. Wu, "Analytical criterion for amplitude death in [24] nonautonomous systems with piecewise nonlinear coupling," Physical Review, vol. 89, no. 4, 2014.
- [25] V. Bertram, Practical Ship Hydromechanics, Oxford: Butterworth-Heimann, 2012.
- [26] J. T. Tuitman, "Hydro-elastic response of ship structures to slamming induced whipping," [PhD Doctoral dissertation, Delft University of Technology], 2010.
- W. E. Cummins, "The Impulse Response Function and Ship Motions," Hydromechanics Laboratory Research and [27] Development Report, 1962.
- F. Remy, B. Molin and A. Ledoux, "Experimental and numerical study of the wave response of a flexible barge," in 4th International Conference on Hydroelasticity in Marine Technology, Wuxi, China, 2006.
- D. Xia, J. W. Kim and R. C. Ertekin, "On the hydroelastic behavior of two-dimensional articulated plates," Marine Structures, vol. 13, pp. 261-278, 2000.
- A. Hikai and H. Omori, "On the prediction of the flow and water quality change due to a mega-float installation," [30] in 22nd Meeting of the US-Japan Marine Facilities Panel, Washington, USA, 1998.
- X. Che, D. Wang, M. Wang and Y. Xu, "Two-dimensional hydroelastic analysis of very large floating structures," [31] Journal of Marine Technology, vol. 29, no. 1, pp. 13-24, 1992.
- [32] J. N. Newman, "Wave effects on deformable bodies," Journal of Applied Ocean Research, vol. 16, pp. 47-59, 1994.
- Q. J. Shi, D. I. Xu, H. C. Zhang and Y. S. Wu, "Optimized stiffness combination of a flexible-base hinged connector for very large floating structures," Journal of Marine Structures, vol. 60, pp. 151-164, 2018.
- J. Ding, C. Tian, Y. S. Wu, X. F. Wang, X. L. Liu and K. Zhang, "A simplified method to estimate the hydroelastic responses of VLFS in the inhomogeneous waves," Journal of Ocean Engineering, vol. 172, pp. 434-445, 2019.

 [35] R. P. Gao, Z. Y. Tay, C. M. Wang and C. G. Koh, "Hydroelastic response of very large floating structures with a flexible line connection," Journal of Ocean Engineering, vol. 38, pp. 1957-1966, 2011.
- Q. Shi, H. Zhang and D. Xu, "Design of a flexible-base hinged connector for very large floating structures," [36] Madrid, Spain, 2018.
- Y. Lu, H. Zhang, Y. Chen, Q. Shi and Y. Zhou, "A new type of connection with optimum stiffness configuration [37] for very large floating platforms," Journal of Engineering for the Maritime Environment, pp. 1-15, 2021.
- T. Utsunomiya, E. Watanabe and R. Eatock Taylor, "Wave response analysis of a box-like VLFS close to a breakwater," Lisbon, Portugal, 1998.
- J. A. Pinkster, A. Fauzi, Y. Inoue and S. Tabeta, "The behaviour of large air cushion supported structures in waves," Fukuoka, Japan, 1998.
- [40] J. L. F. van Kessel, "Air-cushion supported mega-floaters," [PhD Doctoral dissertation, Delft University of Technology], 2010.
- K. Takagi, K. Shimada and T. Ikebuchi, "An anti-motion device for a very large floating structure," Journal of [41] Marine Structures, vol. 13, pp. 421-436, 2000.
- H. Ohta, T. Torii, N. Hayashi, E. Watanabe and T. Utsunomiya, "effect of attachment of a horizontal/vertical plate on the wave response of a VLFS," Honolulu, USA, 1998.
- [43] R. P. Gao, C. M. Wang and C. G. Koh, "Reducing hydroelastic response of pontoon-type very large floating structures using flexible line connector and gill cells," Engineering Structures, vol. 52, pp. 372-383, 2013.
- [44] Y. Cheng, C. Ji, G. Zhai and G. Oleg, "Fully nonlinear numerical investigation on hydroelastic responses of a floating elastic plate over variable depth sea-bottom," Journal of Marine Structures, vol. 55, pp. 37-61, 2017.
- K. Kada, T. Fujita and K. Kitabayashi, "Stress analysis for structurally discontinuous parts in a mega-float [45] structure," Journal of Offshore and Polar Engineering, vol. 12, no. 1, pp. 48-55, 2002.
- E. Watanabe, T. Utsunomiya and S. Tanigaki, "A transient response analysis of a very large floating structure by finite element method," Journal of Structural and Earthquake Engineering, vol. 15, no. 2, pp. 155-163, 1998.